

Analyst

Accepted Manuscript



This is an *Accepted Manuscript*, which has been through the Royal Society of Chemistry peer review process and has been accepted for publication.

Accepted Manuscripts are published online shortly after acceptance, before technical editing, formatting and proof reading. Using this free service, authors can make their results available to the community, in citable form, before we publish the edited article. We will replace this *Accepted Manuscript* with the edited and formatted *Advance Article* as soon as it is available.

You can find more information about *Accepted Manuscripts* in the [Information for Authors](#).

Please note that technical editing may introduce minor changes to the text and/or graphics, which may alter content. The journal's standard [Terms & Conditions](#) and the [Ethical guidelines](#) still apply. In no event shall the Royal Society of Chemistry be held responsible for any errors or omissions in this *Accepted Manuscript* or any consequences arising from the use of any information it contains.

Cite this: DOI: 10.1039/c0xx00000x

www.rsc.org/xxxxxx

ARTICLE TYPE

Manipulating inter pillar gap in pillar array ultra-thin layer planar chromatography platforms†

Nichole A. Crane^a, Nickolay V. Lavrik^b, and Michael J. Sepaniak^{*,a}

Received (in XXX, XXX) Xth XXXXXXXXX 20XX, Accepted Xth XXXXXXXXX 20XX

DOI: 10.1039/b00000

An advantage of separation platforms based on deterministic micro- and nano-fabrication, relative to traditional systems based on packed beds of particles, is exquisite control of all morphological parameters. For example, with planar platforms based on lithographically-prepared pillar arrays the size, shape, height, geometric arrangement, and inter pillar gap can be independently adjusted. Since inter pillar gap is expected to be important in determining both resistance to mass transfer in the mobile phase as well as flow rate, which influences the mass transfer effect and axial diffusion, we study herein the effect of reducing inter pillar gaps on capillary action-based flow and band dispersion. Atomic layer deposition is used to narrow the gap between the pillars for photo-lithographically defined pillar arrays. The plate height of gap-adjusted arrays is modeled based on predicted and observed flow rates. A reduction in flow rate with smaller gaps hinders efficiency in the modeled case and is correlated with actual separations. A conclusion is drawn that simultaneously reducing both the gap and the pillar diameter is the best approach in terms of improving chromatographic efficiency.

Reduction of the dimensions of liquid phase separation systems has been pursued for decades,¹ both in the overall dimensions of the systems (e.g., packed capillaries and open channel systems)²⁻⁵ and in the size of the packing materials (e.g., core shell packing with < 3 μm diameters).⁶⁻⁹ Desmet and coworkers have pioneered a reduced separation approach involving pillar arrays in narrow channels.¹⁰ The Sepaniak group has pursued the pillar arrays for chemical separations (PACS) approach as well and shown advantages of reducing the dimensions of the pillars and inter pillar gaps, both in enclosed pressure driven chips and open planar systems driven by capillary action.¹¹⁻¹² The latter open systems with pillar diameters typically of 2 μm diameter and 4 μm pitch provided surprisingly fast capillary action based flow and plate heights of ≤ 2 μm . Herein we describe the outcome of further reducing the inter pillar gap to determine if the scaling trends in flow and dispersion (plate height) continue.

Advantages of enclosed systems have been documented by Desmet et al. and, similarly, for open systems have been discussed by Kirchner et al.^{1, 12, 13} In summary, nearly perfect ordered pillar arrays exhibit less flow resistance than traditional packed and monolithic columns.^{11, 14} Studies show that pillar arrays wick faster than traditional TLC, reducing molecular diffusion, and have better mass transfer due to the pillar dimensions being substantially smaller than TLC bed particles. Plate heights were significantly smaller than for TLC.¹² Typically, the open planar format chips range from 3 cm x 3 cm to ≤ 0.5 cm x 3 cm allowing the separation media to be portable to on site testing. The separation systems are reusable to help offset production costs and require small sample volumes.

According to the Van Deemter equation, perfectly ordered arrays are expected to reduce plate height significantly and even reduce the eddy-dispersion term to near zero. Due to these advantages, fabrication of these ultra-thin layer separation platforms is a realistic approach for manufacture even with the moderate expense. Recently, a metal dewetting procedure for the fabrication of pillar arrays has further reduce costs.¹⁵⁻¹⁶

However, disadvantages do exist for PACS as they inherently exhibit several shortfalls. PACS when formed via photolithography¹² contain a non-retentive surface. In order to correct for this surface, researchers have employed depositing silicon oxide layers via plasma enhanced chemical vapor deposition (PECVD).¹⁷⁻¹⁸ Other attempts at creating more surface area for PACS have been with electrochemical anodization to create a mesoporous silicon layer.¹⁹ Recently, our group has deposited porous silicon oxide (PSO) on pillar array surfaces using a room temperature PECVD protocol.^{13, 20} The PSO layer allows for faster wicking capabilities, super hydrophobicity (contact angle > 150 $^\circ$), enhanced fluorescence brightness, and chemically selective transport.²¹

An area of interest with PACS is the ability to obtain smaller inter pillar gaps (smaller than 2.0 μm). Many research facilities including universities only have access to mid-UV lithography which allows for the replication of the mask with larger features.²²⁻²³ Using atomic layer deposition (ALD), silicon oxide is conformally deposited onto silicon pillars which cause the pillars to increase in diameter and decrease the inter pillar gap. This in turn can reduce plate height according to the C_M term in the Van Deemter equation (see below). This research is devoted to examining the performance of inter pillar gaps with decreasing dimensions of 1.1 μm , 0.8 μm , and 0.5 μm , along with a more retentive separation media created to increase the surface area. Capillary action is used within the studies described due to the simplicity for planar chromatography solvent development.

In order to determine the best inter pillar gaps to fabricate a solvent wicking model reported by Mai et al. was employed.²⁴ Mai et al. concludes that wicking ability can be controlled by simply changing the geometry of a textured surface. Since performance of capillary action driven systems is very dependent on flow rate, the model provides predictive insights. However, the predictive model does not include surface roughness (addition of PSO) or any evaporation effects, causing the model to not fully depict the outcome of the experimental results.

Fabrication of 2D-Pillar Arrays with Reduced Dimensions

Lithographically Fabricated Pillar Arrays. The pillar arrays used in this study were initially fabricated using a procedure previously reported by Kirchner et al.¹² A CAD program is used to define the pillar pattern, and a Heidelberg LW, Model DWL66

laser writer (Center for Nanophase Materials Science, Oak Ridge National Laboratory, Oak Ridge, TN), is used to create an initial chrome mask. Following, a double layer of positive photoresist (lift-off resist LOR-1A overcoated by positive tone photoresist 955CM-2.1, MicroChem Corp.) was added to the top of a silicon wafer. The pattern for the arrays was made using a Quintel Inc. contact aligner designed to mask off the non-pillared areas which are then etched. Using UV light, holes were formed in the positive photoresist where the pillars are created. Approximately 15 to 20 nm of chromium was deposited onto the wafer to act as the etchant mask, after which the remaining photoresist is removed leaving areas of non-etched chromium (i.e., the pillar tops). A Bosch™ process was performed to generate pillars with a height of ~20 μm (system 100 Plasma Etcher, Oxford

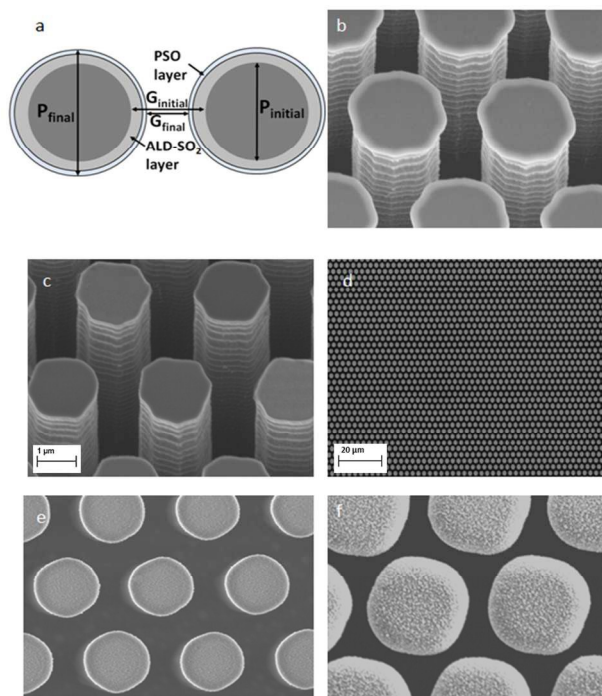


Figure 1: Stages of depositions on pillar arrays; (a) schematic diagram of the depositions of silicon dioxide performed with ALD and PECVD where depositions ranged from 50 nm PSO to 300 nm ALD with 50 nm PSO; (b) SEM of original pillar arrays without a chrome etch (c) SEM of original pillar arrays with a chrome etch; (d) low resolution SEM image of 1.9D1.1G gapped chips; (e) magnified SEM image of 1.9D1.1G gapped chips; (f) magnified SEM images of 2.5D0.5G gapped chips.

Instruments). The wafers were then scribed and cleaved into individual 0.5 cm by 3 cm pillar array chips prior to differing deposition amounts of silicon oxide via ALD and PECVD. All pillar arrays were functionalized with n-Butyldimethylchlorosilane ($\geq 97\%$, Acros Organics) to enhance hydrophobicity of the substrate.²⁵ Figure 1 provides images of the stages of the processing.

Pre-treatment of Pillar Arrays. Before any depositions are conducted the pillar arrays have excess fluoropolymer and chrome from the fabrication process. Fabrication of pillar arrays relies on anisotropic etching of silicon using well established reactive ion etching in a fluorine-based plasma (System 100 Plasma Etcher, Oxford Instruments). This Bosch™ processing step involves plasma polymerization of C_4F_8 precursor gas and is associated with condensation of Teflon-like fluoropolymer on sidewalls and tops of the resulting pillars. Such fluoropolymer deposits consist of predominantly linear $(CF_2)_n$ chains characterized by a low cross-linking degree.²⁶ In order to remove

the fluoropolymer we expose samples to high intensity oxygen plasma on the plasma etcher instrument for 10 min using a recipe that combines 2000 W of inductively coupled plasma and 20 W of capacitively coupled plasma.

This oxygen plasma cleaning procedure is followed by wet etching of the residual chromium masking layer (present on top of the pillars) for 30 s using CR-14S (Cyantek Corp.) The CR14S etchant is based on a mixture of ceric ammonium nitrate and acetic acid with thickening and stabilizing additives. Thorough rinsing with DI water and blow drying of samples with filtered nitrogen concludes the cleaning/etching step (see Figure 2). This cleaning step does not ensure that all of the fluoropolymer and chrome are removed, nor is it entirely necessary to remove all due to large depositions performed on the pillar arrays with ALD and PECVD.

Controlling Inter-Gap Dimensions. In order to create different gap distances, differing amounts of silicon dioxide was deposited using ALD in order to receive an extremely uniform deposition on all pillar tops and sidewalls. The original 0.5 cm by 3 cm chips had pillar heights of ~20 μm, diameters of 1.8 μm, and gaps of 1.2 μm. One additional case was tested where the original pillar diameter started out smaller (~0.8 μm). Four different gap cases were fabricated. In order to increase surface area of the chips to achieve an optimum separation platform, the PECVD was used at room temperature to deposit a PSO layer. Desmet et al. has shown that the porous silicon layer adequately increases surface area in ordered arrays and therefore allows more surface silanols for bonding with the with the n-Butyldimethylchlorosilane reverse phase stationary phase used herein.^{19, 27}

For cases I-III, the 1.8 μm diameter chip was used and case IV the 0.8 μm diameter chip was used. Cases II-IV were put in the ALD instrument for a 150 nm deposition of uniform silicon dioxide. After the first deposition, Case II and IV chips were removed from the instrument and Case III chips remained for another 150 nm deposition. Depositing 150 nm of silicon oxide on the sidewalls of pillars causes the gap to close by 300 nm. At the end of the atomic layer depositions, all chips were placed in the PECVD chamber to deposit 50 nm of PSO. This low temperature PECVD protocol produces PSO that has been shown to be suitable for chromatography.¹³ This caused another 100 nm closing of the gap. The goal was to create a 1.9 μm diameter/1.1 μm gap chip (1.9D 1.1G), a 2.2 μm diameter/0.8 μm gap chip (2.2D 0.8G), a 2.5 μm diameter/0.5 μm gap chip (2.5D 0.5G), and a 1.2 μm diameter/0.8 μm gap chip (1.2D 0.8G).

Measuring Flow and Band Dispersion

To measure flow each 3 cm x 0.5 cm pillar array chip was sealed in a 20 mL vial with ~7 mL of the respective solvent (acetonitrile or 2-propanol) for a period of 5 minutes to allow the chamber to reach equilibrium. The vial is fitted with a plunger in order to introduce the chip to solvent once the chamber/vial reaches equilibrium. The pillar array chip is adhered to the plunger via double-sided tape. A video is recorded of the solvent flow for each gap size and analyzed with imageJ software to ensure precise distance measurements with time.

For band dispersion experiments an analyte spot of ~200 μm diameter was administered to the pillar array via an HPLC syringe. The analyte spotted was a mixture of 10^{-6} M sulfur rhodamine, 10^{-5} M coumarin 540A, and 10^{-5} M coumarin 120 in 60:40 methanol:water. The spot was typically administered 3 mm from the bottom of the array to avoid dipping the analyte directly into the mobile phase. Band dispersion measurements and a separation could be performed simultaneously. The analyte spot was measured before and after a separation was performed using

50:50 methanol:water as the mobile phase. Separations were performed using the 20 mL vial as described above. Separations were analyzed at 2 and 4 minute development times.

To measure band dispersion, separated bands are imaged with a fluorescence microscope and once saved are opened with ImageJ software. On the fluorescence microscope the field of view at the 10x microscope objective is 1400 μm . In the ImageJ software the image is manually set to a field of view of 1400 μm . For exact band measurements an area of the band is highlighted and an intensity graph is created. Tangential lines from a best-fit Gaussian are used to determine separated band width. Where the tangential lines hit the x-axis estimates the width of the band (4σ). As is common for planar chromatography, spot-based bands are only roughly Gaussian giving some error with the determination of band variance. The average of multiple runs and measurements were made to minimize this effect.

Modeling of 2D-Pillar Arrays with Reduced Dimensions

While factors that contribute to plate height, H , are extremely complex in planar chromatography, the treatment by Guiochon is generally regarded as comprehensive and is based on the validity of the Van Deemter equation (Equation 1) that is common to HPLC theory.²⁸

$$H = A + \frac{B}{v} + (C_s + C_m)v \quad [1]$$

Generally plate height is dependent on eddy diffusion, A , longitudinal diffusion, B , which is influenced by the mobile phase velocity (v) and the resistance to mass transfer in both the stationary and mobile phases, C_s and C_m , respectively. Expansion of the Van Deemter equation to include the parameters that influence plate height is shown in Equation 2.

$$H = 2\lambda d_p + \frac{2\gamma D_M}{v} + \frac{qk'd_s^2v}{(1+k')^2 D_s} + \frac{\omega d_p^2v}{D_M} \quad [2]$$

In this equation the critical particle diameter is represented by d_p , the chromatographic capacity factor is k' , the average film thickness of the stationary phase is d_f , the diffusion coefficients for the solute in the stationary and mobile phases are D_s and D_m , and independent factors that are specific to the quality of the column packing include q , λ , γ , ω .¹²⁻¹³

The Eddy diffusion term, also known as the multipath effect, is disregarded in our theory because the pillar arrays have uniform morphology.¹² Mass transfer in and out of the porous layer (C_s) is layer thickness dependent.¹⁹ Since our 50 nm thickness is at least an order of magnitude less than porous layer packings that have become popular in HPLC,²⁹ and the porous pillar arrays of De Malsche and coworkers prepared by an electrochemical anodization process,¹⁹ we expect that our C_s contribution is relatively minor. Moreover, it should be relatively constant as we change morphological parameters while keeping a constant porous layer thickness. Therefore, we estimate plate height based on only the B and C_m terms in the Van Deemter equation as shown below (Equation 3) with typical literature values for γ and ω inserted.^{17, 30-31} In traditional packed bed chromatography with laminar flow, the gaps between particles is linked to d_p ; smaller values produce smaller gaps and those gaps govern resistance to mass transfer in the mobile phase. In contrast, the deterministically-fabricated pillar arrays used herein have independent control over pillar diameter and inter pillar gaps (G) and thus we replace d_p with G in the equation.

$$H = \frac{2(0.5)D_M}{v} + \frac{0.02G^2v}{D_M} \quad [3]$$

In HPLC the first (B) term above is simply compensated by increasing the flow rate (with concomitant higher pressure). This of course increases the second (C_m) term and necessitates a decrease in particle size. Rapid flow is essential for high

efficiency in planar (e.g., TLC) separations. Equation 4 describes the effects of parameters on flow in traditional planar chromatography.

$$\mu_f^2 = K_0 t d_p \left(\frac{\gamma'}{\eta}\right) \cos \theta \quad [4]$$

In this equation, μ_f is the displacement of the solvent front, d_p is the diameter of the stationary phase particles, γ' represents the surface tension, η the dynamic viscosity and θ , is the contact angle of the mobile phase. A dilemma arises in that small particles needed to improve C_m will exacerbate the B term as flow rate decreases. However, for pillar array platforms the permeability constant (K_0) is considerably larger than for

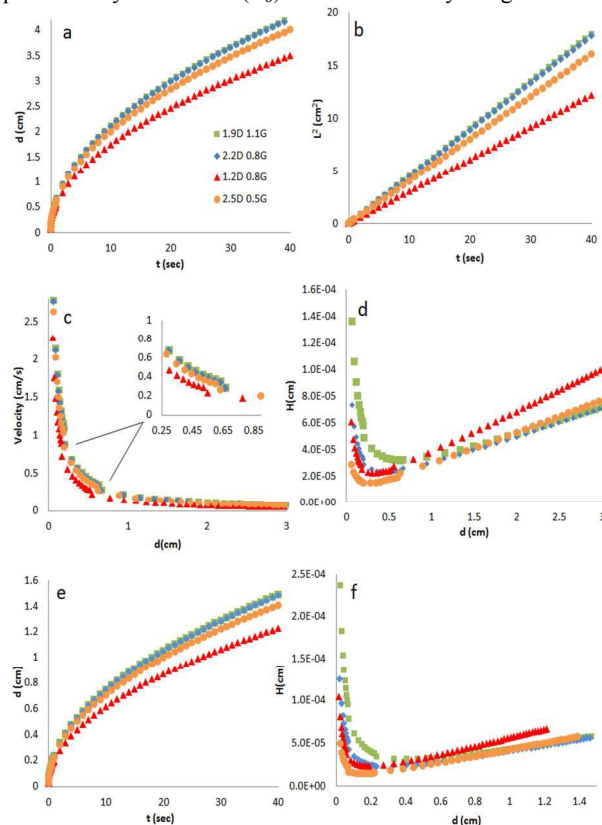


Figure 2: Predictive solvent flow of acetonitrile (a)-(d) and 2-propanol (e)-(f); (a) distance versus time of four different morphologies; (b) position squared versus time to illustrate linearity; (c) distance versus velocity; (d) efficiency plot to determine optimum gapped scenario; (e) distance versus time and (f) efficiency plot for 2-propanol.

traditional flat beds of packing materials and hence flow is greater.^{11,12} Moreover, Equation 4 may not be adequate to describe flow in deterministically-fabricated pillar arrays wherein independent and precise control of morphology is possible.

To predict the effects of pillar array geometry on flow, hence efficiency, we use the semi-empirical model developed by Mai et al. for ordered arrays of silicon pillars.²⁴ This predictive flow model is based on the geometrical parameters of the fabricated substrate, experimentally measured solvent-substrate contact angles, and literature values for solvent viscosity and surface tension.^{21, 24} The H term is then estimated (Equation 3) for these nano-scale arrays using a typical diffusion coefficient of $5.0\text{E-}6$ cm^2/s in acetonitrile and $1.0\text{E-}6$ cm^2/s for the more viscous 2-propanol (Figure 2).

Equation [4] points to a greater flow for larger particles, but it should be noted that this is a consequence of larger inter particle gaps and less flow resistance. The equation does not reflect the total situation in our pillar arrays or as it pertains to Figure 2a where both pillar diameter and gap are controlled independently. The three pillar arrays that started with 1.8 μm pillar diameters and used ALD/PECVD to close the gap follow the order of 1.9D1.1G > 2.2D0.8G > 2.5D0.5G with respect to flow rate but predicted to flow fairly similarly (see figure) despite the significant reduction in gap size through the series. It appears that the increase in both surface area and diameter (1.9D1.1G (18.4cm²), 2.2D0.8G (21.3cm²), 2.5D0.5G (2.42cm²), and 1.2D0.8G (26.1cm²), see SI Table 2), enhances contact wetting, and continuous-nature (smaller gaps to traverse, more open tube-like) as the inter-pillar gaps decrease through the series compensates for the increase in flow resistance. The pillar array that started with ~1 μm diameter, i.e., 1.2D0.8G, is predicted to move significantly slower. This system has a higher surface area than the larger diameter 0.8G counterpart, but is less continuous in nature. It is worth contrasting the arrays with isolated pillars to a packed bed through which flow involves particles with many points of contact. In previous work the arrays were shown to flow significantly faster (higher K_o) than packed beds.¹² It is the conversion of the predicted flow to a relationship between position of the front on the array and the flow velocity (Figure 2c) which is critical in predicting the effects of array morphology and solvent properties on chromatographic efficiency via Equation 3. Figure 2c demonstrates a predicted rapidly diminishing flow over the first 1 cm of the array which continues at positions greater than 1 cm but at a lower, nearly linear, rate of decrease. These flows are plotted for acetonitrile which has a favorable γ'/η ratio for rapid flow.

The question arises what type of band dispersion dominates the determination of plate height as the solvent front proceeds along the array based on these predications. The situation is grafted in Figure 2d. At larger solvent front positions, where axial diffusion is most problematic, the slower 1.2D0.8G system exhibits larger plate heights with the three larger pillar diameter series performing nearly equally (note the linear slopes past 1 cm). Nearer the origin where flow is rapid and resistance to mass transfer may be significant the smallest gap (2.5D0.5G) system produces the lowest plate heights and optima nearest the origin; although there is a significant upturn in all the plots near the origin. Optimum velocities and development distances (point at which B and Cm terms are equal) for each morphology are presented in SI. In the predicted scenario, decreasing inter pillar gap causes the optimum velocity to increase (see Table 1 in SI). The corresponding distance at each optimum velocity then decreases. The main observation with these predictions is that closing the gap is important in reducing plate height because it reduces the C_m term but does not reduce wicking velocities as much as conventional TLC when d_p is decreased. The 2-propanol system (Figure 2e,f) moves slower but also has a smaller expected D_M . The SI provides a treatment for determining the resolution for test cases at positions along the array.

Performance of 2-D Pillar Arrays with Reduced Dimensions

The predictions discussed above fall short of mimicking our experimental arrays in that we have a 50 nm thick PSO layer on the pillar sidewalls, which are fabricated in a triangular arrangement not square as assumed by the predictive flow model. The predictive flow profile also does not consider evaporation. Thus the model is a guide and permits discussion of the effects of morphology on 2-D planar platform separation performance but

cannot be expected to exactly represent experimental data. Figure 3 is the experimental analog of the modeling shown in Figure 2. As expected the largest inter pillar gap scenario shows the most rapid flow of the pillar arrays that began with the same 1.8 μm diameter (1.9D1.1G). The 2.2D0.8G and 2.5D0.5G scenarios have slower flow profiles in that order, which is consistent with the predictive data. However, the experimental data shows a greater difference in flow velocity over this series than that of the predictive flow studies, presumably due to the increased surface area of the PSO layer which is not considered in the model. In addition the flow rates are approximately a factor of two slower than that of the modeled data. The result is that that the up-turn of the H versus position d plots is not observed (Figure 3d). The 1.2D 0.8G case, where the pillar diameters started smaller than the other pillar array cases displays behavior that contrast of what the model predicts. The predictions are relevant for all pillar arrays that begin with the same pillar diameter. Again, this may reflect the effect of the PSO layer.

Separations with Sub- μm Dimension Pillar Arrays

The efficiency treatment in the previous section considers experimental flows coupled with assumptions regarding the parameters in Equation 3. We now present actual experimental separations with analytical metrics.

As can be seen in Figure 4, the separations that occur at a 2 minute development typically see more inconsistent results likely

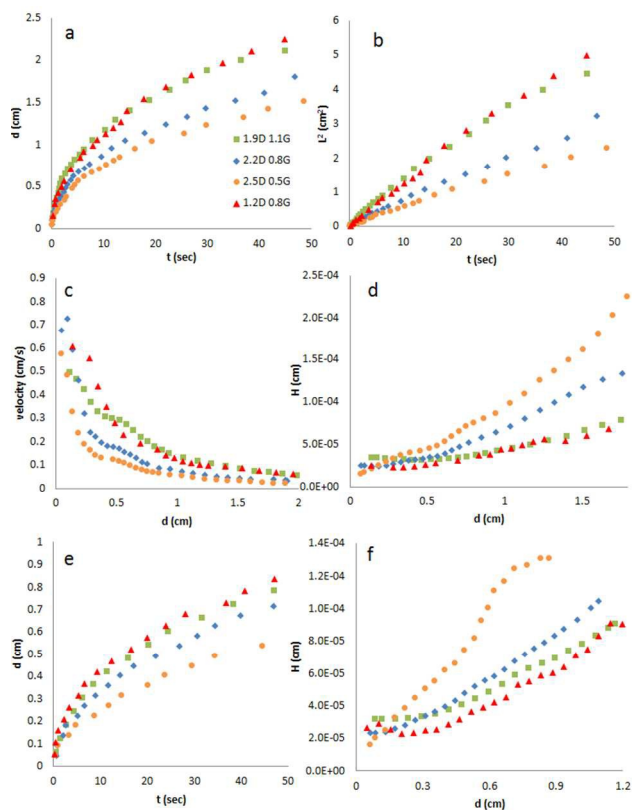


Figure 3: Experimental solvent flow of acetonitrile (a)-(d) and 2-propanol (e)-(f); (a) distance versus time of four different inter pillar gap distances; (b) position squared versus time to illustrate linearity; (c) distance versus velocity; (d) efficiency plot to determine optimum gapped scenario; (e) distance versus time and (f) efficiency plot for 2-propanol.

due to the fast velocity solvent flow being abruptly stopped and the non-automated separation process. The 4 minute development separations experienced less bandwidth variability and exhibited comparable plate height results as the solvent flow rate-based plate height plots shown in Figure 3. Plate height values in

Figure 3d,f show that the 2.5D 0.5G performs the worst, which is consistent with the experimental values seen in Figure 4. This large plate height is not a matter of large bandwidth but rather due to the small distance traveled of the mobile phase (see SI Table 3). It is encouraging that the trends in separations-based plate heights seen in Figure 4a and especially b (4 minutes) mimics the trends seen in Figure 3d,f. However, it should be noted that the plate heights in Figure 3 are based on experimental flow rates and Equation 3. Conversely, non-van Deemter factors that can influence efficiency and reproducibility such as spot size, spot solvation kinetics, and band drying post separation are operative in the experimental separations-based efficiencies expressed in Figure 4.

In summary, predicted flow profiles (Figure 2) showed similar results to that of the experimental flow profiles (Figure 3) except in the case of the smaller diameter pillars studied herein. The small diameter pillar case was predicted to flow with the slowest velocity but experimentally had a similar flow profile to the largest gap scenario. This variation in results may be attributed to the predicted flow data not correcting for the increased surface

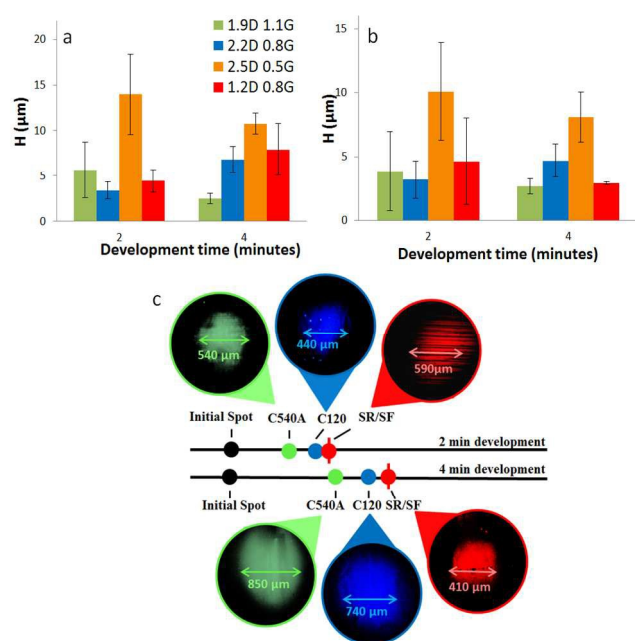


Figure 4: Average plate height values for (a) C540A separated bands and (b) C120 separated bands. (c) Example of a 2 minute development versus a 4 minute development on a 2.2D 0.8G chip.

area of the porous shell-core pillars or the evaporation rate of the solvents used. Since it is the inter pillar gap that is expected to influence resistance to mass transfer in the mobile phase there was motivation to reduce that gap. Such a change to smaller gaps is also expected to increase viscous drag that we hoped would be compensated by a greater surface area that drives the wicking process. However, the increase in surface area did not adequately compensate, flow rates decreased, and efficiency suffer due to molecular diffusion band dispersion (see both Figures 3 and 4). The smaller pillar diameter studied had the greatest surface area and performed well in terms of wicking flow rates and efficiency, thereby providing motivation for using fabrication methods that can scale both the pillars and gaps into the nanometer range.⁶

Acknowledgements

This material is based upon work supported by the [National Science Foundation](#) under Grant No. 1144947 with the University of Tennessee, Knoxville. A portion of this research was

conducted at the [Center for Nanophase Materials Sciences](#), which is sponsored at Oak Ridge National Laboratory by the Scientific User Facilities Division, Office of Basic Energy Sciences, U.S. Department of Energy.

Notes and references

^aDepartment of Chemistry, University of Tennessee, Knoxville, TN, 37996, USA. ^bCenter for Nanophase Materials Sciences, Oak Ridge National Laboratory, Oak Ridge, TN, 37830, USA.

†Electronic Supplementary Information (ESI) available.

- Desmet, G.; Eeltink, S., *Analytical Chemistry* **2012**, *85* (2), 543-556.
- Chervet, J. P.; Ursem, M.; Salzmann, J. P., *Analytical Chemistry* **1996**, *68* (9), 1507-1512.
- Gritti, F.; Guiochon, G., *Journal of Chromatography A* **2012**, *1244* (0), 184.
- Eeltink, S.; Dolman, S.; Swart, R.; Ursem, M.; Schoenmakers, P. J., *Journal of Chromatography A* **2009**, *1216* (44), 7368-7374.
- Zhou, F.; Lu, Y.; Ficarro, S. B.; Webber, J. T.; Marto, J. A., *Analytical Chemistry* **2012**, *84* (11), 5133-5139.
- Fekete, S.; Fekete, J., *Journal of Chromatography A* **2011**, *1218* (31), 5286-5291.
- Bruns, S.; Grinias, J. P.; Blue, L. E.; Jorgenson, J. W.; Tallarek, U., *Analytical Chemistry* **2012**, *84* (10), 4496-4503.
- Gritti, F.; Guiochon, G., *LC-GC North America* **2012**, *30*, 586+.
- DeStefano, J. J.; Langlois, T. J.; Kirkland, J. J., *Journal of Chromatographic Science* **2008**, *46* (3), 254-260.
- De Malsche, W.; De Bruyne, S.; Op De Beek, J.; Sandra, P.; Gardeniers, H.; Desmet, G.; Lynen, F., *Journal of Chromatography A* **2012**, *1230* (0), 41-47.
- Taylor, L. C.; Kirchner, T. B.; Lavrik, N. V.; Sepaniak, M. J., *Analyst* **2012**, *137* (4), 1005-1012.
- Kirchner, T. B.; Hatab, N. A.; Lavrik, N. V.; Sepaniak, M. J., *Analytical Chemistry* **2013**, *85* (24), 11802-11808.
- Kirchner, T. B.; Strickhouser, R. B.; Hatab, N. A.; Charlton, J. J.; Kravchenko, I. I.; Lavrik, N. V.; Sepaniak, M. J., *Analyst* **2015**, *140* (10), 3347-3351.
- Gzil, P.; Vervoort, N.; Baron, G. V.; Desmet, G., *Journal of Separation Science* **2004**, *27* (10-11), 887-896.
- Charlton, J. J.; Jones, N. C.; Wallace, R. A.; Smithwick, R.; Bradshaw, J. A.; Kravchenko, I. I.; Lavrik, N. V.; Sepaniak, M. J., *Analytical Chemistry* **2015**, *87*, 6814-6821.
- Charlton, J. J.; Lavrik, N. V.; Bradshaw, J. A.; Sepaniak, M. J., *Journal of Applied Materials and Interfaces* **Submitted**.
- Lavrik, N. V.; Taylor, L. C.; Sepaniak, M. J., *Lab on a Chip* **2010**, *10* (8), 1086-1094.
- Gustafsson, O.; Mogensen, K. B.; Kutter, J. P., *ELECTROPHORESIS* **2008**, *29* (15), 3145-3152.
- De Malsche, W.; Clicq, D.; Verdoold, V.; Gzil, P.; Desmet, G.; Gardeniers, H., *Lab on a Chip* **2007**, *7* (12), 1705-1711.
- Fekete, S.; Fekete, J., *Journal of Chromatography A* **2011**, *1218* (31), 5286-5291.
- Charlton, J. J.; Lavrik, N.; Bradshaw, J. A.; Sepaniak, M. J., *ACS Applied Materials & Interfaces* **2014**, *6* (20), 17894-17901.
- Callewaert, M.; De Beeck, J. O.; Maeno, K.; Sukas, S.; Thienpont, H.; Ottevaere, H.; Gardeniers, H.; Desmet, G.; De Malsche, W., *Analyst* **2014**, *139* (3), 618-625.
- De Malsche, W.; Op De Beeck, J.; De Bruyne, S.; Gardeniers, H.; Desmet, G., *Analytical Chemistry* **2012**, *84* (3), 1214-1219.
- Mai, T. T.; Lai, C. Q.; Zheng, H.; Balasubramanian, K.; Leong, K. C.; Lee, P. S.; Lee, C.; Choi, W. K., *Langmuir* **2012**, *28* (31), 11465-11471.
- Wallace, R. A.; Charlton, J. J.; Kirchner, T. B.; Lavrik, N. V.; Datskos, P. G.; Sepaniak, M. J., *Analytical Chemistry* **2014**, *86* (23), 11819-11825.
- Lindroos, V.; Tilli, M.; Lehto, A.; Motooka, T., *Micromachining technologies in MEMS*. In *Handbook of Silicon Based MEMS Materials and Technologies*, Second Edition ed.; Elsevier, Ed. 2015.
- Malsche, W. D.; Gardeniers, H.; Desmet, G., *Analytical Chemistry* **2008**, *80* (14), 5391-5400.
- Guiochon, G.; Siouffi, A., *Journal of Chromatographic Science* **1978**, *16* (10), 470-481.
- Tanaka, N.; McCalley, D. V., *Analytical Chemistry* **2015**.
- Deiningner, G., *Chromatographia* **1976**, *9* (6), 251-254.
- Myers, P., *Chromatographia* **2003**, *57* (11-12), 834-834.

1
2
3
4
5
6
7
8
9
10
11
12
13
14
15
16
17
18
19
20
21
22
23
24
25
26
27
28
29
30
31
32
33
34
35
36
37
38
39
40
41
42
43
44
45
46
47
48
49
50
51
52
53
54
55
56
57
58
59
60